1962

A magnetic film low frequency parametric amplifier

Glenn Ellsworth Fanslow
Iowa State University

A MAGNETIC FIIM IOW FREQUENCY PARAMETRIC AMPLIFIER

by

Glenn Ellsworth Fanslow

A Dissertation Submitted to the
Graduate Faculty in Partial Fulfillment of
The Requirements for the Degree of
DOCTOR OF PHILOSOPHY

Major Subject: Electrical Engineering

Approved:

Signature was redacted for privacy.

In Charge of Major Work

Signature was redacted for privacy.

Head of Major Department

Signature was redacted for privacy.

Dean of Graduate College

Iowa State University
Of Science and Technology
Ames, Iowa

1962

TABLE OF CONTENTS

I. INTRODUCTION

A. The Noise Problem

The ultimate usable sensitivity of a practical amplifier is limited by the random fluctuations or "noise" that the amplifier adds to the signal, since any signal weaker than this noise will be masked or hidden. Thus, the effect of noise is to interfere with the detection and amplification of low level signals. In the early years of amplifier development the need for low noise amplifiers was not great. However, as interests began to expand in the fields of communications, servomechanisms, instrumentation and other areas dealing with low level signals there was a natural increase of interest in noise phenomena and the design of less noisy devices. The purpose of this study was to develop and analyze just such a device; a low noise, low frequency, magnetic film parametric amplifier.

Nearly every component in an electric amplifier is a source of noise. A resistor produces thermal noise, bulk ferromagnetic materials introduce Barkhausen noise, and vacuum tubes have flicker noise, partition noise, shot noise, etc. As a consequence these and the other components that are the building blocks in electric amplifiers also serve to limit an amplifier's sensitivity. It is not the purpose here to cover all of the aspects of this problem, but just to discuss briefly some of the noises that act as limiting factors in the detection and amplification of low level signals.

B. Noise in Small-Signal Amplifiers

Vacuum tubes and transistors are the most familiar amplifying devices in use today and their inherent noise has been investigated rather extensively. The physical nature of some of the sources of noise in these devices is now fairly well understood and formalized, and research is being carried on in an attempt to correlate the remainder of the noise(s) being generated with some physical process(es). All noise(s) whose mechanism(s) is (are) unknown is (are) classified as flicker noise, while the other noises present are known by specific names such as shot noise, Johnson noise, partition noise, etc.

Shot noise is present in both vacuum tubes and semiconductors and is of a statistical nature. In vacuum tubes it is the effect of the random emission of electrons from a heated surface. Shot noise in semiconductors resembles that in vacuum tubes in that it occurs only if a voltage is applied, however, in semiconductors charges appear and disappear in the material itself. A portion of the shot noise in semiconductors is due to the fluctuations in the processes of carrier creation and annihilation, while the remainder is attributed to the fluctuations in the diffusion process.

Flicker noise also limits the sensitivity of small signal amplifiers. Its effect is present in both tubes and transistors and it is most noticeable at low frequencies. The general tendency of this noise is for it to have a noise-frequency spectrum that varies as an inverse function of frequency and it is often called $\frac{1}{f}$ noise. While the exact mechanism of this (these) noise(s) is not fully understood, Van Der Ziel (11) discusses a

theory by Schottky for vacuum tubes that postulates the random arrival and departure of foreign atoms at the cathode surface. This theory agrees reasonably well with experimental results. Flicker noise in transistors is explained by Fonger (2) in terms of two actions, one being a slow variation in the probability of electron-hole-pair generation and recombination at the surface and the other a leakage noise associated with electrical breakdown in the high field region at the edge of the collector junction.

Thermal noise, or Johnson noise as it is sometimes called, can be caused by different mechanisms; shot effect, black body radiation, the random interaction between the free electrons and the vibrating ions in a given conducting medium, etc. It would be wrong to conclude that all thermal noise results from any single effect even though one may be predominant. Actually the classification of the different thermal sources is not generally important because the interest is in the amount of noise from a circuit and not its specific origin.

Nyquist (5) shows that the effect of thermal noise in the frequency range df in an impedance $Z = R + jX$ is equivalent to an emf in series with a noiseless impedance. The mean square value of the noise voltage is

$$\overline{e^2} = 4kTRdf \qquad (1)$$

where R is the effective series resistance of the impedance, Z, at the frequency in question, K is Boltzmann's constant, T is the temperature in degrees Kelvin and df is the small frequency bandwidth over which the open circuit voltage is measured. A proof is given in Appendix A.

Barkhausen noise is associated with the discontinuous and irreversible domain boundary movements that occur when the direction of magnet-

ization is varied in materials that have many magnetic domains. This may be illustrated by using the model of the domain structure of a single crystal of iron as shown in Figure 1. In Figure 1A the position of the domain boundaries with zero field is shown by the solid line. The domain structure has been formed to minimize the energy associated with the localized fields due to the effect of free poles induced in the specimen. Since the energy associated with free poles is relatively large, it is necessary that the component of magnetization normal to the domain boundaries be continuous as far as possible. For the minimum energy condition then there are seen to be no free poles on the 180° (vertical) boundary. The closure domains at the ends of the crystal also form in such a way as to minimize the energy due to free poles. Since the area of the closure domain is generally small compared with the area of the 180° boundary, the effects of the closure domains may be assumed to be negligible. A change in the magnetic field causes the movement of the 180° boundary across the crystal to position x. If the crystal is perfect, without any non-magnetic inclusions or other defects the movement will be smooth and no Barkhausen noise will be generated. When the crystal is strained or it has non-magnetic inclusions present at a boundary the direction of the component of magnetization normal to the domain boundary is no longer continuous and free poles are produced. The presence of inclusions results in a retardation of the movement of sections of the domain wall, Figure 1B. The motion of the retarded sections of the boundary will be discontinuous and will proceed in jumps producing Barkhausen noise. The Barkhausen effect is small and it is not often noticed, but its presence would be apparent on a hysteresis curve if the curve were pictured in sufficient

Figure 1. Model of the domain structure in a single crystal of iron. (A) Position of 180° (vertical) boundary in a field H is shown. Solid line shows boundary for H = 0. (B) Retardation of a section of the boundary with the production of free poles.

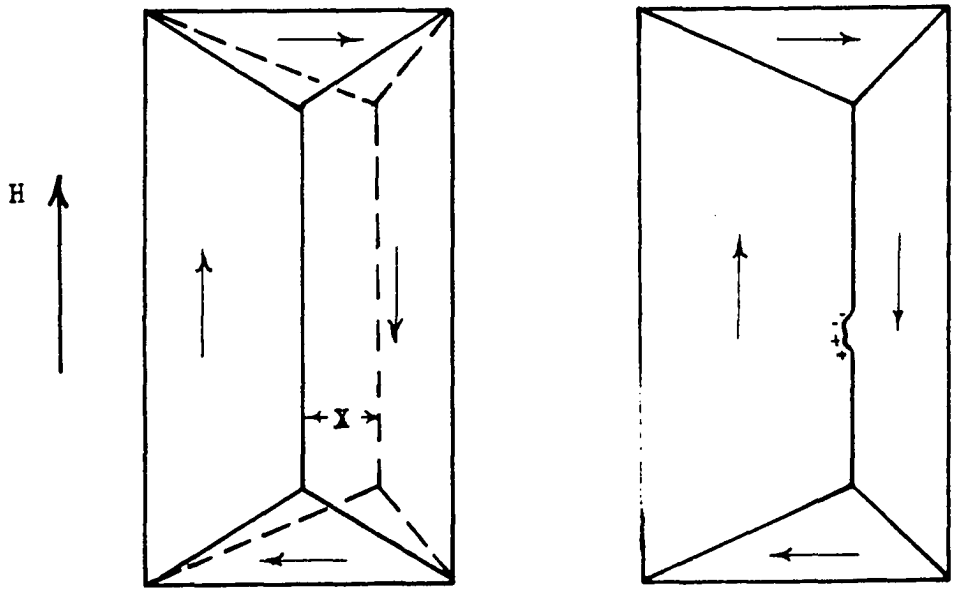

A B

detail. On the curve, changes in magnetization as a function of field applied would proceed in a series of steps rather than smoothly as it is generally shown. Tebble (10) shows that these step changes in magnetization are dependent upon the position of the inclusions, the width of the inclusions, and the length of the section of the domain wall that is retarded. Biorci and Pescetti (1) say that the Barkhausen effect produces a pulse that may be represented by an exponential curve having a time constant of approximately 10^{-4} second. Their study utilized the random superposition of these pulses in determining that the spectral density of Barkhausen noise is constant up to 1 kc and that it decreases rapidly thereafter. Since the distribution of sizes of Barkhausen discontinuities in bulk and thin film magnetic materials is similar, as has been shown by Ford and Pugh (3), one would expect the same type of noise from each. Williams and Noble (12) indicate that Barkhausen noise is the limiting factor in the signal level that may be amplified by present magnetic amplifier methods.

One of the most successful methods of avoiding the zero drift and noise problems that arise in the attempt to amplify low-level low-frequency signals is the up-conversion of the d-c or low frequency signal to a higher frequency where it undergoes conventional a-c amplification. The means for doing this has mainly been mechanical: choppers, vibrating capacitors and similar devices. The tendency in the past has been to rely on this method rather extensively because it was very familiar and has generally produced good results. The shortcomings of mechanical modulators are that their sampling rates are low, they are subject to mechanical failure, and their contacts opening and closing are a source of noise.

Other devices that have received a considerable amount of attention recently as being low in noise content are maser amplifiers and parametric amplifiers using electron beams, variable reactance diodes, etc. The applications of these amplifiers have generally been in the UHF and microwave regions and they will not be considered here.

C. The Thin Magnetic Film Balanced Modulator

The application of thin magnetic films in balanced modulator circuits was proposed by Read (6) and investigated by Samuels (9). They show that the thin magnetic film lends itself rather readily to operation at frequencies from d-c to several hundred kilocycles and can be made to be rather sensitive. This study was begun to gain more knowledge of the use of thin magnetic films in the area of low-level, low-frequency low-noise amplification.

Since the thin magnetic film balanced modulator is a reactive device it should not be a source of shot noise or the $\frac{1}{f}$ noise found in vacuum tubes and transistors. Essentially, in the balanced modulator application, the thin magnetic film exists as a single magnetic domain and as a consequence should not be a source of Barkhausen noise. Therefore, the only noise limiting the sensitivity of the thin film balanced modulator would come from the thermal noise being generated in the resistances of the circuit.

II. THE AMPLIFIER

A. Power Gain

The advantage of using nonlinear reactance elements in the up-conversion of low-level low-frequency signals is that, in addition to producing a higher frequency a-c signal, a large power gain is available. This concept is not new. It has been used extensively in magnetic and dielectric amplifier applications. Basically the small signal input to this type of device is used to control large amounts of energy that is supplied from some a-c source. This action is similar to that of the more conventional vacuum tube amplifier where the small voltage changes on the grid of the tube control large amounts of energy supplied from the d-c source, i.e. the battery or B^+ supply. While the vacuum tube acts as a nonlinear resistance in the circuit supplied by the d-c source, the magnetic or dielectric amplifier acts as a nonlinear reactance in the circuit supplied by the a-c source. There are, however, differences in these two rather similar amplifying devices. The output of the amplifier supplied by a d-c source is generally a replica of the input, while the output of the reactor modulator is not. It generally occurs at a different frequency. Also the properties of energy transfer, sensitivity, bandwidth, etc. associated with reactor modulators are not as well known as those of the more familiar amplifiers whose energy is supplied from a d-c source. The general energy relations which govern nonlinear reactor modulators have been derived by Manley and Rowe (4). In their discussion they show that the average powers at the different frequencies in nonlinear reactor modulators are related by two independent equations. Salzberg (8)

has developed the Manley-Rowe relations for the particular case of three frequencies, one being at the signal frequency, one being at the carrier frequency, and the third being the sum or difference of signal and carrier frequencies. When the load is only responsive to the sum and difference frequencies the relations are:

$$\frac{-P_3}{f_3} = \frac{P_2}{f_2} = \frac{+P_1}{-f_1} \qquad (2)$$

where: f_1 is the signal frequency

f_2 is the local oscillator or carrier frequency

$f_3 = (f_1 \pm f_2)$ is the output sum or difference frequency

P_1, P_2, P_3 are the powers at the frequencies f_1, f_2 and f_3 with the negative sign to indicate power absorption.

From equation 2 the power gain obtainable is

$$(G_p)_{23} = \frac{\pm f_3}{f_1} = \frac{\pm f_1 \pm f_2}{f_1} \qquad (3)$$

When $f_2 >> f_1$ the gain approaches the ratio of the carrier frequency to that of the signal frequency. It must be realized that this is the theoretical power gain and that allowances may have to be made for losses in the nonlinear element, coupling losses etc.

B. Operation

A single magnetic domain thin film is illustrated in Figure 2A. $\vec{M}$ is the saturation magnetization vector of the material having a preferred or rest direction that is normally determined by the uniaxial anisotropy field. This direction is induced during the formation of the film by

Figure 2. Schematic representation of a single domain thin film (A) and the utilization of the thin film in a balanced modulator configuration (B).

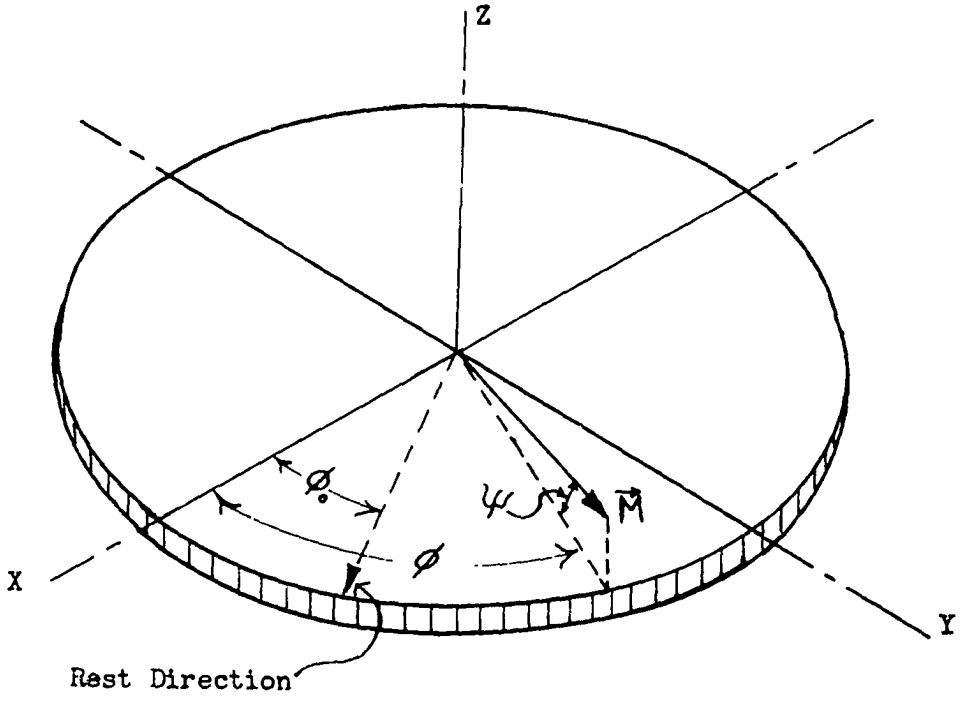

A

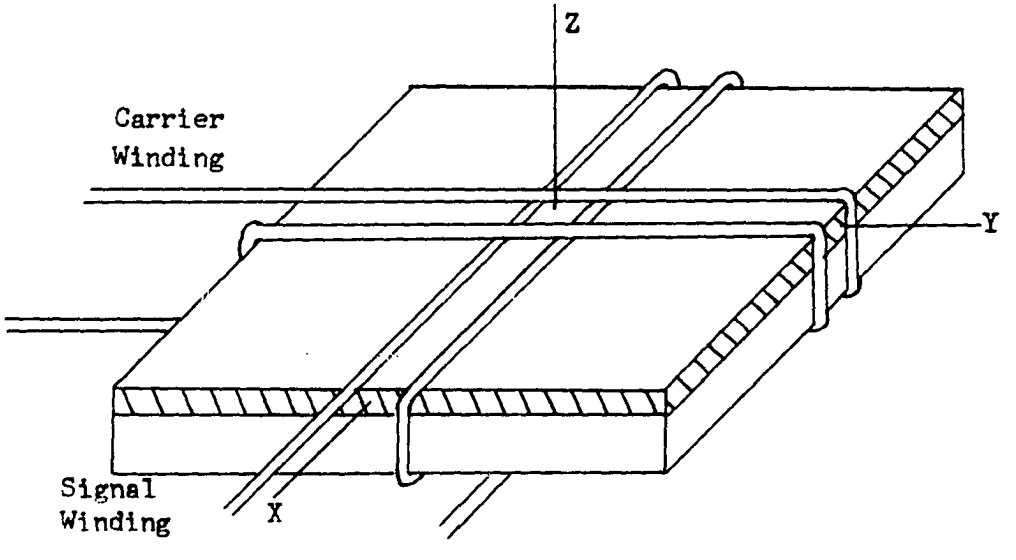

B

applying an external field parallel to the plane of the film. It is possible to rotate $\vec{M}$ through the angle ϕ in the plane of the film by the application of an external magnetic field with a component that is perpendicular to the rest direction. The torque resulting from the $\vec{M} \times \vec{H}$ cross product would tend to rotate $\vec{M}$ out of the plane of the film through the angle ψ . However, large demagnetizing fields normal to the plane of the film are produced by any vertical movement of $\vec{M}$, and ψ remains very small. When $\psi = 0$ there is no demagnetizing field and $\vec{M}$ would still have a tendency to rotate out of the plane of the film. Read and Pohm (7) show that ψ will remain small for frequencies up to several hundred megacycles and that it is possible to assume that $\vec{M}$ only moves in the plane of the film at lower frequencies.

Figure 2B shows the thin magnetic film as it was used in the balanced modulator circuit used by Samuels (9). This particular configuration lends itself rather readily to an explanation of the balanced modulator operation which was given by Samuels and which is followed here in order to build the necessary background.

The carrier winding is placed on the film with its magnetic axis parallel to the rest direction of the film. Two windings are placed on top of the carrier winding (only one being pictured for clarity) with their magnetic axes perpendicular to the rest direction of the film. One of these will be the signal or modulation winding while the other will be the output winding. With these two windings lying perpendicular to the carrier winding there is no mutual inductance between them and the carrier winding.

Operation is most easily described by picturing what takes place with

a d-c signal input. A d-c bias current I_b and a carrier current i_c at a fixed angular frequency of ω_c are caused to flow in the carrier winding. A d-c signal current flowing in the modulation winding will produce a field h_m which will rotate the magnetization vector $\vec{M}$ through an angle ϕ. When this occurs the magnetization vector $\vec{M}$ is no longer perpendicular to the axis of the output winding and a flux is established that links this winding. In addition, $\vec{M}$, no longer parallel to the axis of the carrier winding, will feel the effects of the fields induced by the carrier currents. The alternating field will cause $\vec{M}$ to be rocked around some equilibrium value of the angle ϕ, resulting in a constant variation of the magnetic flux linking the output winding. The voltage induced in this winding will be at the frequency of the carrier and have a magnitude largely dependent on the equilibrium value of ϕ. The small signal currents flowing in the modulating winding will vary ϕ and thus control a-c voltages induced in the output winding. A degree of nonlinearity with respect to the modulation current is to be expected, but this can be avoided by limiting ϕ to small angles.

A sinusoidal current flowing in the modulation winding will cause $\vec{M}$ to rotate around the rest direction of the film and the carrier current will be rocking it around its instantaneous "equilibrium" position. The voltage induced in the output winding will then be that of suppressed carrier double sideband modulation. This is illustrated in Figure 3A.

The analysis has assumed, and the operation requires, that the magnetic axis of the carrier winding is parallel with the rest direction of the film and that the output and signal windings are perpendicular to the rest direction of the film. If this is not the case true balanced modulator

Figure 3. Illustration of a balanced (A) and an unbalanced (B) waveform from the modulator.

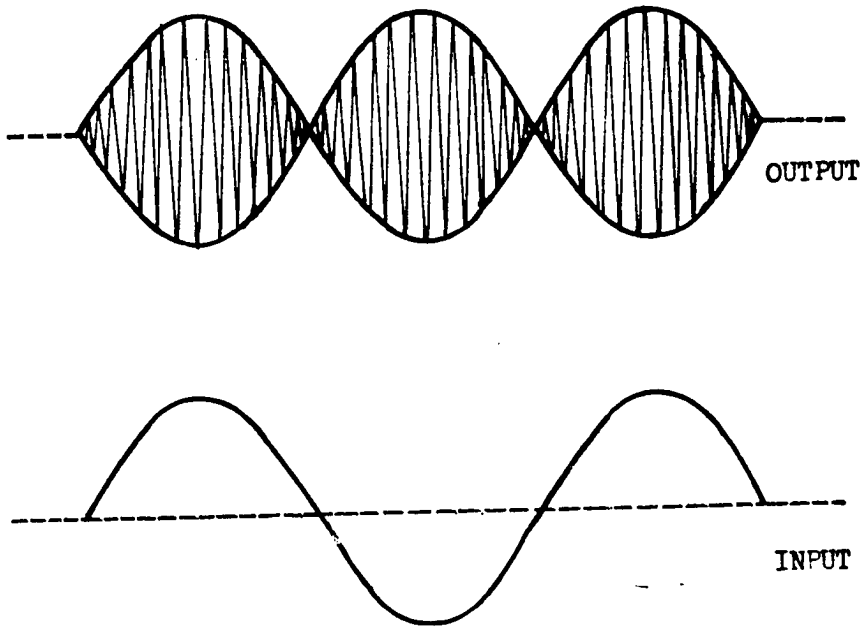

A

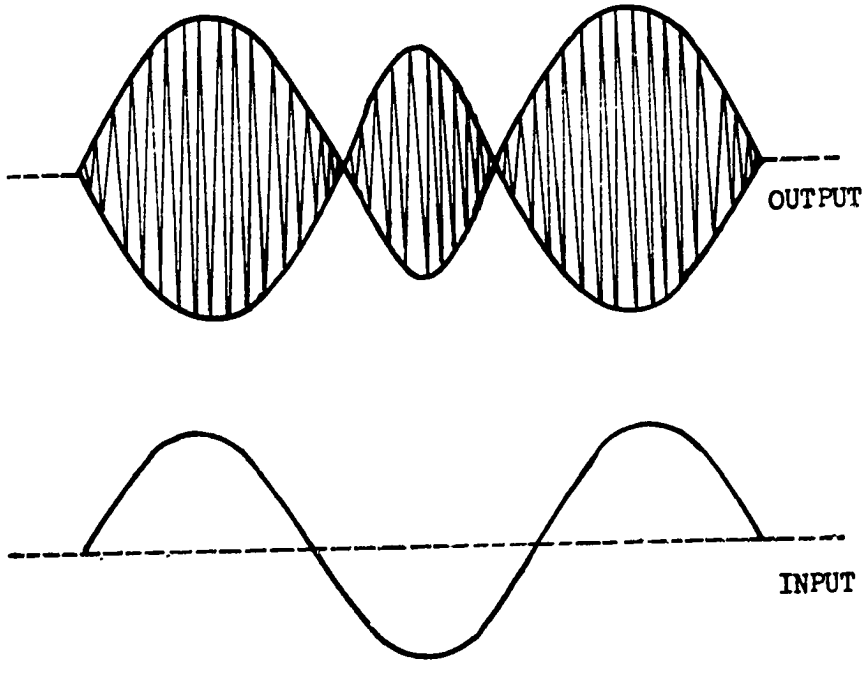

B

operation will not occur; a voltage at the carrier frequency will be induced in the output winding with no modulation signal present. It is possible to introduce an external magnetic field or to move the output winding to reduce zero-modulation induced carrier frequency voltages to zero, but this only results in a loss in balance in the output. Because of the anisotropy of the film, the equilibrium angle of rotation, ϕ, of the magnetization vector, M, will be different for positive and negative modulation signals of the same magnitude. This effect is illustrated in Figure 3B.

C. Construction

Many hours of analytical and experimental work are associated with magnetic thin films and their applications. They, like other devices before them, have to go through the formative period as laboratory models until they can be engineered and fabricated to perform their specific function. Except for some computer oriented applications, thin film devices are generally still in the laboratory or developmental stage.

The most difficult problem in the actual building of a thin film balanced modulator is the proper alignment of the windings with respect to the easy direction of the film. Some methods of accomplishing this are given by Samuels (9) and others are described later. Another problem that complicates the design is the interwinding capacitance that exists between the carrier and the output windings. Unless this capacitance can be made small the carrier signal will be coupled through to the output.

The construction of the thin film balanced modulator developed for

this study is shown in Figure 4. The magnetic film used was not the same shape or even the same type as that described previously. The earlier films used in balanced modulator circuits were vacuum deposited on glass substrates and it was difficult to determine the rest direction of magnetization accurately and then to wind the necessary coils around the film properly. The film used in this investigation had been electroplated on a length of small copper wire with the rest direction of magnetization lying circumferential to the axis of the wire. By using the inner copper wire to act as a shorted turn carrying the carrier currents the requirement that the magnetic axis of the carrier winding should be parallel to the rest direction of the film was met. The output winding was made up of two coils wound on a small capillary tube. The modulation winding was also made in two coils, but these were wound on coil forms with holes through their center. Then, with the plated wire through the center of the capillary tube and the coil forms slipped down over the outside of the capillary, the axes of the output and modulation coils were perpendicular to the rest direction of the magnetization.

Some advantages were realized with this model. By using two coils with their windings in opposite directions it was possible to cancel out some of the misalignment effects that still existed. Another feature of this particular configuration was the reduction of the interwinding capacitance. This was due to the short length of the carrier winding, the relatively low voltage differential between the ends of this winding, and the shielding afforded by the magnetic film that was between the carrier and output windings. A disadvantage of this model was the loss that resulted from the fact that the output and modulation windings were

Figure 4. Illustration of the magnetic thin film parametric amplifier.

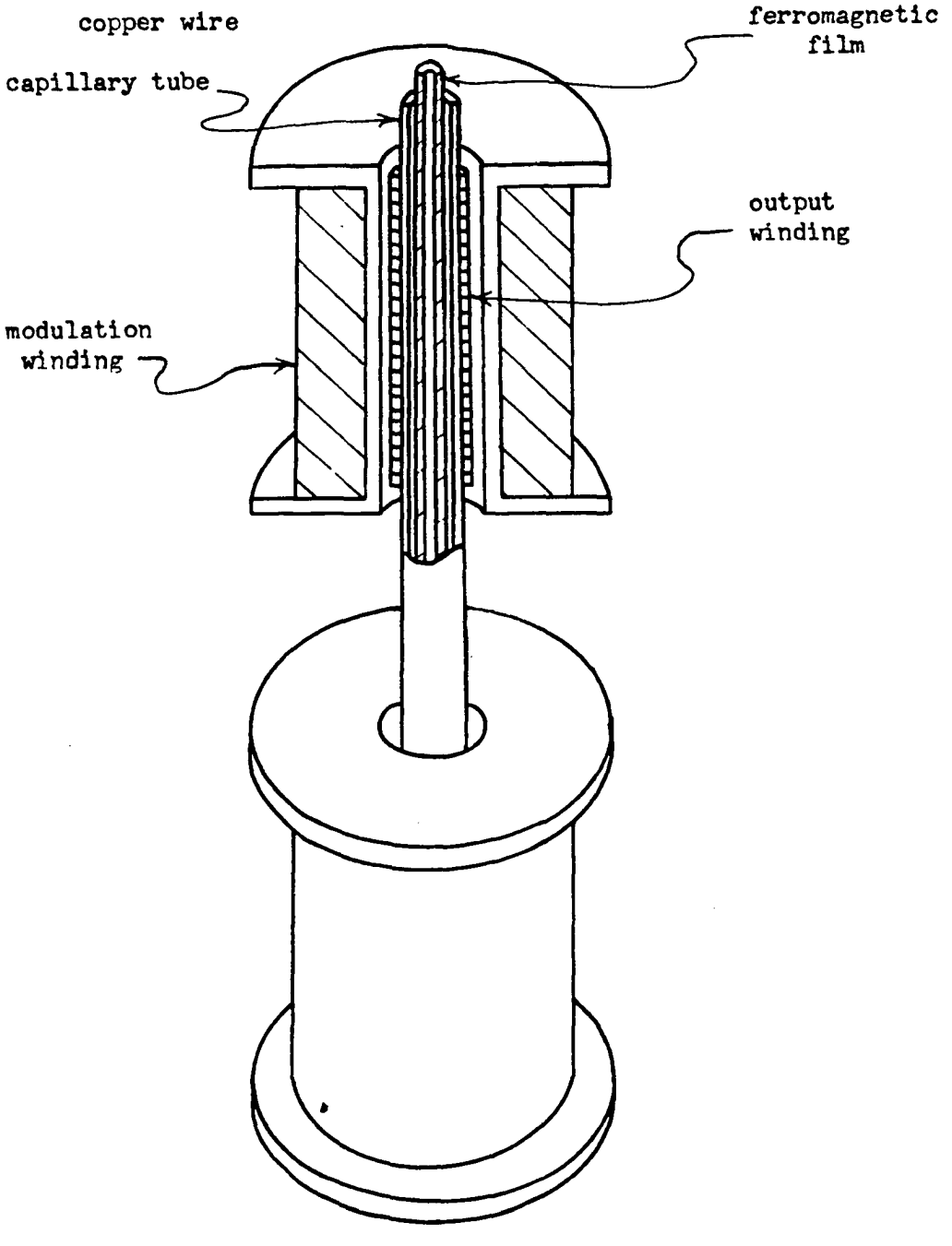
copper wire
ferromagnetic film
capillary tube
output winding
modulation winding

not coupled tightly to the film, but were separated by air, glass etc. In future models it may be possible to "pot" the plated wire, so it will not be subject to magnetostrictive effects, and then to wind the output and modulation coils on this.

D. Analysis

Salzberg (8) shows that in the up-converter a small amount of power at the signal frequency, f_s, controls a large amount of power at the carrier frequency, f_c. This power appears as useful output power at the sum, f_+, and difference, f_-, frequencies. The power output at the sum frequency is the sum of the power inputs at f_s and f_c, while the power output at the difference frequency is the power output from f_c minus the power input to f_s. In the latter case the input to f_- will be large while the input to f_s will be small. Effectively the power is transferred, inductively, from the a-c source to the circuit containing a nonlinear inductor.

The inductance of the output winding of the balanced modulator can be derived for low frequency applications where quasi-static conditions exist. First consider the expression for the magnetic flux density $\vec{B}$ at a point in a magnetic domain

$$\vec{B} = \mu_o \vec{H} + \vec{M} \qquad (4)$$

where μ_o is the permeability of free space, $\vec{H}$ is the total magnetic field intensity at the point and $\vec{M}$ is the saturation magnetization of the material. For the balanced modulator configuration given in Figure 2B the external field, $\vec{h}$, applied to the system consists of $\vec{a}_x h_c$ and $\vec{a}_y(h_s + h_o)$ where $\vec{a}_x$ and $\vec{a}_y$ are unit vectors along the coordinate axes

and h_c, h_s, and h_o are the magnitudes of the carrier, signal, and output fields respectively. The flux density that will be directed along the axis of the output winding will be

$$B = \mu_o(h_s + h_o) + M \sin \phi \tag{5}$$

Assume that the flux density is uniform over the areas in question; the film, the air gaps between the windings and the wire on which the film has been plated. Now let A be the cross-sectional area of the output winding and A_f be the cross-sectional area of the film. The expression for the flux in the output winding is

$$\Phi = A\,\mu_o(h_s + h_o) + A_f M \sin \phi \tag{6}$$

By considering the film's magnetic energy density Read (6) has solved for sin ϕ for the quasi-static condition and found it to be expressible as

$$\sin \phi = \frac{(h_s + h_o)\,M}{2K\left[1 + \dfrac{h_c M}{2K\,(\cos \phi)}\right]} \tag{7}$$

where K is the anisotropy constant of the material. Letting $h_s M/2K = h'_s$, $h_o M/2K = h'_o$, and $h_c M/2K = h'_c \sin \phi$ becomes

$$\sin \phi = \frac{h'_s + h'_o}{1 + \dfrac{h'_c}{\cos \phi}} \tag{8}$$

Substituting for sin ϕ in equation 6 and grouping terms the flux is

$$\Phi = \left[A\mu_o h_o + \frac{MA_f h'_o}{1 + \dfrac{h'_c}{\cos \phi}}\right] + \left[A\mu_o h_s + \frac{MA_f h'_s}{1 + \dfrac{h'_c}{\cos \phi}}\right] \tag{9}$$

The total flux in the output winding is seen to be the flux produced by

the output winding that is linking the output winding, Φ_{oo}, and flux produced by the signal winding that is linking the output winding, Φ_{os}. For the case where ϕ is small so that $\cos \phi \cong 1$; and by multiplying by N, the number of turns of the output coil, the flux linkages are found to be

$$\lambda_o = NA\mu_o h_o + \frac{NMA_f h'_o}{1 + h'_c} + NA\mu_o h_s + \frac{NMA_f h'_s}{1 + h'_c} \qquad (10)$$

The fields induced by the carrier, signal and output windings are related to the currents in these windings by constants. Therefore, let $h'_c = k'_c i_c$, $h'_s = k'_s i_s$, $h'_o = k'_o i_o$, $h_c = k_c i_c$, $h_s = k_s i_s$ and $h_o = k_o i_o$, and λ_o becomes

$$\lambda_o = i_o \left[NA\mu_o k_o + \frac{NMA_f k'_o}{1 + h'_c} \right] + i_s \left[NA\mu_o k_s + \frac{NMA_f k'_s}{1 + h'_c} \right] \qquad (11)$$

It is convenient here to let $L_o = NA\mu_o k_o$, $\alpha = \frac{A_f M k'_o}{A\mu_o k_o}$, $\eta = NA\mu_o k_s$, and $\beta = \frac{A_f M k'_s}{A \mu_o k_s}$ to obtain

$$\lambda_o = i_o L_o \left[1 + \frac{\alpha}{1 + h_i} \right] + i_s \eta \left[1 + \frac{\beta}{1 + h'_c} \right] \qquad (12)$$

The inductance of the output winding can then be written

$$L_o = \frac{\lambda_{oo}}{i_o} + \frac{\lambda_{os}}{i_s} = L_o \left(1 + \frac{\alpha}{i + h'_o}\right) + \eta \left(1 + \frac{\beta}{1 + h'_c}\right) \qquad (13)$$

Similar logic may be used to determine the inductance of the signal winding as

$$L_s = \frac{\lambda_{ss}}{i_s} + \frac{\lambda_{so}}{i_o} = L_s \left(1 + \frac{\alpha}{1 + h_c'}\right) + \eta\left(1 + \frac{\beta}{1 + h_c'}\right) \qquad (14)$$

These inductances consist of self and mutual inductances which are made up of an air inductance plus the contribution of the film. The assumptions made in this derivation were that ϕ was small, the flux density was uniform and that the frequency was low so that quasi-static conditions would prevail. With these restrictions the inductance is seen to be only a function of the magnetic field intensity due to the currents in the carrier winding. When these currents cause the inductance to be a time-varying linear quantity, the conditions for the Manley-Rowe power relations exist and the device is capable of transferring power from one frequency to another.

The expression for flux in the output winding assumed currents to be flowing in both the output and the modulation coils. If it is assumed that the current in the output coil is negligible or zero, as in the open circuit case, the flux in the coil becomes

$$\Phi = A \mu_o h_s + A_f M \sin \phi \qquad (15)$$

and the flux linkages can be written as

$$\lambda = NA \mu_o h_s + NA_f M \sin \phi \qquad (16)$$

By letting $NA_fM = \lambda_f$ and remembering that $h_s = k_s i_s$, λ becomes

$$\lambda = (NA \mu_o k_s) i_s + \lambda_f \sin \phi \qquad (17)$$

The term in parenthesis in equation 16 is the η that follows equation 11, and λ_f is defined as the maximum flux linkage contributed by the film. The voltage induced in the output winding will then be

$$e_o = \frac{d\lambda}{dt} = \eta \frac{di_s}{dt} + \lambda_f \frac{d(\sin \phi)}{dt} \qquad (18)$$

This voltage can be thought of as being the sum of two voltages; one induced across an air inductance and the other being contributed by the presence of the film. In order to determine the latter it would be necessary to determine the time rate of change of sin ϕ. Read (6) has derived an expression for the dynamic behavior of the angle ϕ and from this he has developed an expression for the current flow in the transverse winding. This expression can be interpreted as a node voltage equation for a parallel circuit containing several nonlinear elements. The voltage across this parallel circuit is found to be equal to the voltage across the terminals of the inductance due to the presence of the film. One of the nonlinear elements arrived at is identical to the component of the quasi-static inductance of the output winding that is contributed by the magnetic film. In this discussion the film component of the quasi-static inductance is that contributed by the film to the mutual inductance of equation 13. From his results Read (6) arrives at an equivalent circuit, Figure 5A, for the dynamic model of the thin film inductor as seen from the terminals of the input winding. The resultant circuit is arrived at by considering that the air inductance is external to the terminals or is negligibly small and that the winding resistance and interwinding capacitance can be accounted for by placing equivalent R and C components across the terminals.

If appropriate conditions exist it is possible to reduce the equivalent circuit shown in Figure 5A to the "linearized" equivalent circuit of Figure 5B. These conditions are listed by Read (6) as: 1. That the spin resonance of the ferromagnetic electrons occurs at a much higher frequency than any of interest in the balanced modulator. 2. That the

Figure 5. The equivalent circuits of the thin film inductor.
(A) The equivalent circuit for the dynamic model.
(B) The "linearized" equivalent circuit for the quasi-static model.

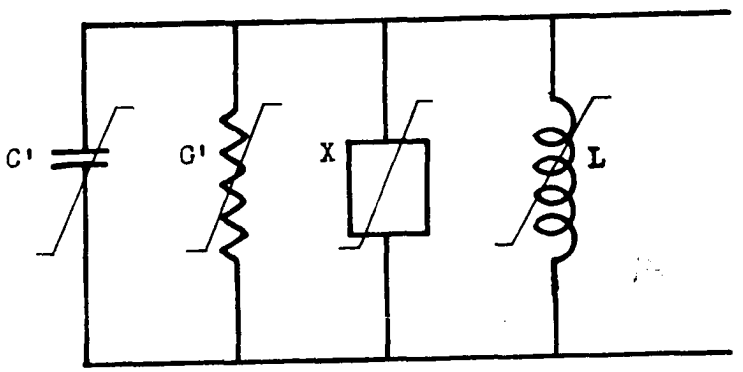

A

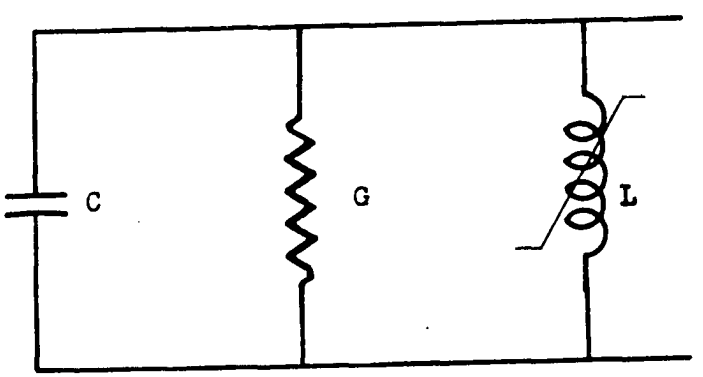

B

air inductance is considered to be in series with the parallel arrangement of the RLC network or that it is assumed to be small and its effects can be absorbed into an equivalent parallel capacitance and inductance at the winding's terminals. 3. That the angle of rotation of the magnetization vector remains considerably less than 90 degrees. 4. A capacitance much greater than the C due to the film and a conductance much greater than the G due to the film must be added externally to be able to consider the conductance and capacitance of the equivalent circuit to be linear.

The "linearized" equivalent circuit was developed by considering the dynamic behavior of the equilibrium angle ϕ. Another approach is to determine the Thevenin equivalent impedance by deriving expressions for the open circuit voltage and the short circuit current that would exist in the output winding of the balanced modulator. This derivation follows.

The position of the magnetization vector, $\vec{M}$, is determined by the externally applied fields and the anisotropy field in the plane of the film. When a d-c modulation current and an a-c carrier current are flowing in the modulation and carrier windings, $\vec{M}$ will be rotated in the plane of the film to an equilibrium angle, ϕ, where it will be rocked about by the time-varying carrier field. If it is assumed that the carrier current is $i_c = I_c \sin \omega_c t$, the output current is $i_o = I_o \sin \omega_c t$, the modulation current is $i_m = I_m$ and the perturbations of $\vec{M}$ about ϕ are small the balancing of forces requires that

$$I_c \sin \omega_c t \; N_c \sin(\phi + \delta \sin \omega_c t) + H_k \sin(\phi + \delta \sin \omega_c t) \cos(\phi + \delta \sin \omega_c t)$$

$$= I_m N_m \cos(\phi + \delta \sin \omega_c t) + I_o \sin \omega_c t \; N_o \cos(\phi + \delta \sin \omega_c t) \quad (19)$$

where the terms, starting from the left, refer to the forces produced by the carrier, anisotropy, modulation and output fields respectively. The term $\delta \sin \omega_c t$ refers to the small perturbation of $\vec{M}$ about ϕ. The replacement of $\sin(\phi + \delta \sin \omega_c t)$ and $\cos(\phi + \delta \sin \omega_c t)$ by their trigonometric identities and the assumptions that $\cos(\delta \sin \omega_c t) \cong 1$ and $\sin(\delta \sin \omega_c t) \cong \delta \sin \omega_c t$ enable one to write

$$\begin{aligned} & N_c I_c \sin \omega_c t (\sin\phi + \delta \sin \omega_c t \cos \phi) \\ & + H_k (\sin \phi + \delta \sin \omega_c t \cos \phi)(\cos \phi - \delta \sin \omega_c t \sin \phi) \\ & = I_m N_m (\cos \phi - \delta \sin \omega_c t \sin \phi) \\ & + I_o \sin \omega_c t \; N_o (\cos \phi - \delta \sin \omega_c t \sin \phi) \end{aligned} \quad (20)$$

Multiplication and equating of coefficients produces for the d-c term

$$H_k \sin \phi = I_m N_m \quad (21)$$

for the $\sin \omega_c t$ term

$$I_c N_c \sin \phi - H_k \delta (\cos^2\phi - \sin^2\phi) = I_o N_o \cos \phi - I_m N_m \delta \sin \phi \quad (22)$$

for the $\sin^2 \omega_c t$ term

$$I_c N_c \cos \phi - H_k \delta \cos \phi \sin \phi = I_o N_o \sin \phi \quad (23)$$

From equation 22 with $I_o = 0$ (the open circuit condition)

$$\delta = - \frac{I_c N_c \sin \phi}{H_k (\cos^2 \phi - \sin^2 \phi) + I_m N_m \sin \phi} \quad (24)$$

and from equation 21

$$\sin \phi = \frac{I_m N_m}{H_k} \quad (25)$$

The open circuit output voltage is

$$e_o = \lambda_f \frac{d \sin(\phi + \delta \sin \omega_c t)}{dt} = \lambda_f \frac{d(\sin \phi + \delta \cos \phi \sin \omega_c t)}{dt}$$

$$= \lambda_f \omega_c \delta \cos \phi \cos \omega_c t \quad (26)$$

from equation 18.

Substitution of δ from equation 24 into equation 26 results in

$$e_o = \frac{\omega_c \lambda_f \cos \phi \, (-I_c N_c \sin \phi) \cos \omega_c t}{H_k (\cos^2 \phi - \sin^2 \phi) + I_m N_m \sin \phi} \tag{27}$$

Under short circuit conditions the fields produced by the time-varying carrier and output currents will be much larger than the d-c modulation field and the anisotropy field of the film. With this thought in mind and the assumption that the perturbations of $\vec{M}$ about ϕ are small it can be said that

$$i_c N_c \sin \phi = i_o N_o \cos \phi \tag{28}$$

for short circuit conditions. Thus, the short circuit output current is

$$i_o = i_c \frac{N_c}{N_o} \frac{\sin \phi}{\cos \phi} = I_c \frac{N_c}{N_o} \frac{\sin \phi}{\cos \phi} \sin \omega_c t \tag{29}$$

and $I_o = I_c \frac{N_c}{N_o} \frac{\sin}{\cos}$.

The ratio e_o (open circuit) to i_o (short circuit) will give the Thevenin equivalent impedance. Switching to phasor form, making some substitutions and simplifying the impedance is

$$Z_o = \frac{\omega_c \lambda_f N_o \cos^2 \phi}{H_k (\cos^2 \phi - \sin^2 \phi) + I_m N_m \sin \phi} \angle 90^\circ \tag{30}$$

If the angle ϕ is small

$$Z_o \cong \frac{\omega_c \lambda_f N_o}{H_k} \angle 90^\circ . \tag{31}$$

It is to be noted that the impedance is entirely inductive, as would be expected since no loss mechanisms were considered, and that it is only a function of the carrier frequency, characteristics of the film and the

number of turns of the output coil squared since $\lambda_f = N_o M A_f$.

With the preceding discussion of the thin film inductor and the attendant assumptions and restrictions in mind it is now possible to develop a theory of its operation in an up-convertor amplifier.

To compute the operating characteristics of the up-converter the circuit shown in Figure 6 will be used. For this development the G and the C of the equivalent circuit for the thin film inductor are omitted. This is permissible in the case of the capacitance because the frequency of operation is much lower than the spin resonance frequency of the ferromagnetic electrons from which it arises. Whether or not the conductance can be omitted depends upon the particular thin film inductor. Since its presence would only change the values of the currents I_s and I_o by a constant, G is omitted for simplicity. The signal circuit is indicated by X_s and R_s together with a filter, f_s, that allows only current at the signal frequency to flow. A similar circuit containing X_o, R_o, and f_o is shown for the output frequencies. Since the two output frequencies are so close to the carrier frequency, it is possible to assume that X_o will represent the reactance seen by both frequencies in the output circuit.

Read (6) shows that the thin film inductor of the form

$$L = \eta(1 + \frac{\beta}{1 + h_c'}) \tag{32}$$

may be written as

$$L = \eta(1 + \frac{a_o}{2} - \frac{a_1}{2} \cos \omega_c t) \tag{33}$$

if the following restrictions are noted: 1. That the carrier current is small. 2. That the carrier current consists of a d-c plus a sinusoidal

Figure 6. Circuit used in the accompanying derivation of the gain from the thin film parametric amplifier.

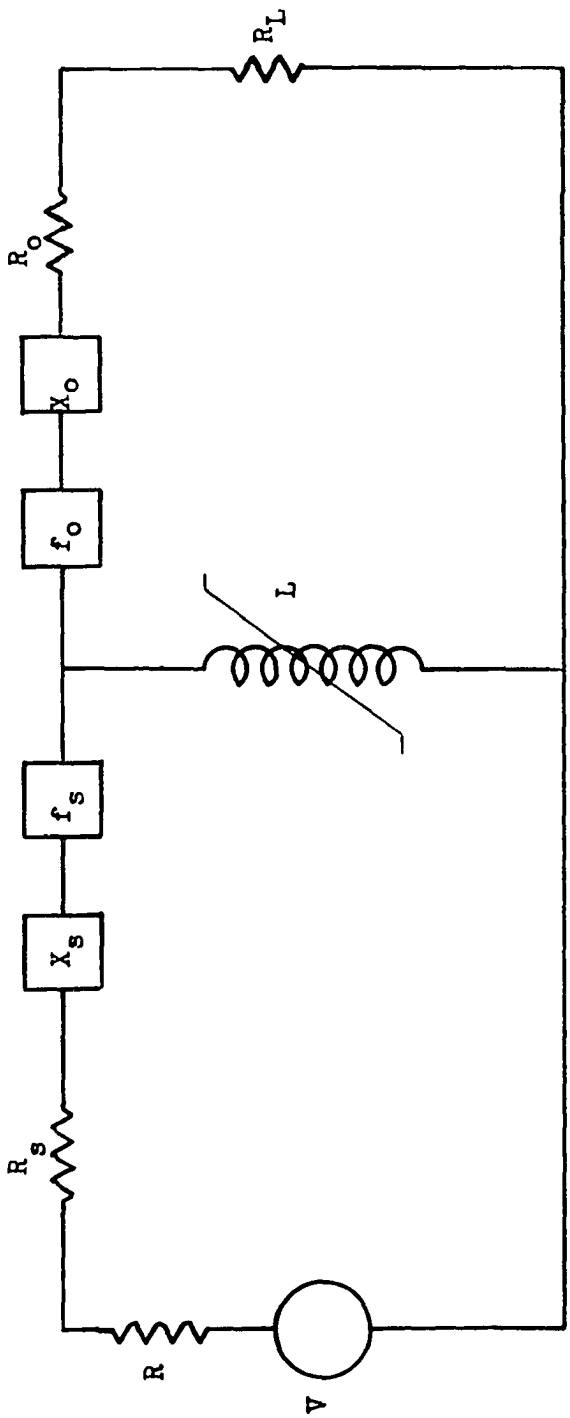
R_L
R_o
X_o
f_o
L
f_s
X_s
R_s
R
V

quantity. Since these restrictions apply in the balanced modulator operation, this expression will be used for inductance in the following derivation. The inductance is seen to be a linear time-varying quantity which can be written

$$L = \eta\left[1 + \frac{a_s}{2} - \frac{a_1}{4}\left(e^{j\omega_c t} + e^{-j\omega_c t}\right)\right] \qquad (34)$$

For the tuned circuit considered the only large voltages which exist across the inductor are at the signal frequency and the sum and difference frequencies. These voltages and the resultant currents through the inductor may be written as

$$v = V_s e^{j\omega_s t} + V_s^* e^{-j\omega_s t} + V_- e^{-j\omega_- t} + V_-^* e^{-j\omega_- t} + V_+ e^{j\omega_+ t} + V_+^* e^{-j\omega_+ t} \qquad (35)$$

$$i = I_s e^{j\omega_s t} + I_s^* e^{-j\omega_s t} + I_- e^{j\omega_- t} + I_-^* e^{-j\omega_- t} + I_+ e^{j\omega_+ t} + I_+^* e^{-j\omega_+ t} \qquad (36)$$

where ω_+ and ω_- are the sum and difference angular frequencies respectively.

The voltage across the inductor is related to the current in it by

$$v = \frac{d\lambda}{dt} = \frac{d\left[L(t)\, i(t)\right]}{dt} \qquad (37)$$

Substitution of the values of current from equation 36 and the value of the inductance from equation 34 into equation 37 produces the following expressions for V_s, V_-^*, and V_+:

$$V_s = j\omega_s\left[\eta' I_s + \eta' I_-^* + \eta_1 I_+\right] \qquad (38)$$

$$V_-^* = -j\omega_-\left[\eta_1 I_s + \eta' I_-^*\right] \qquad (39)$$

$$V_+ = j\omega_+\left[\eta_1 I_s + \eta' I_+\right] \qquad (40)$$

where $\eta' = \eta + \eta\frac{a_0}{2}$ and $\eta_1 = \eta\frac{a_1}{4}$. The differentiation of equation 37

produces some additional harmonic frequencies but these are omitted because they are assumed to be filtered.

Since $V_-^* = I_-^* \left[R_o + R_L + X_o\right]$ and $V_+ = I_+ \left[R_o + R_L + X_o\right]$ it may be shown that

$$I_-^* = I_s \left[\frac{-j\omega_- \eta_1}{R_o + X_o + R_L + j\omega_- \eta^1} \right] \tag{41}$$

$$I_+ = I_s \left[\frac{j\omega_+ \eta_1}{R_o + X_o + R_L - j\omega_+ \eta^1} \right] \tag{42}$$

V_s is also equal to $V - I_s \left(R + R_s + X_s\right)$, therefore, substitution for V_s, I_-^*, and I_+ in equation 38 produces

$$V - I_s \left(R + R_s + X_s\right) = I_s(j\omega_s) \left[\eta^1 + \eta_1^2 \left(\frac{j\omega_+}{R_o+X_o+R_L - j\omega_+ \eta^1} - \frac{j\omega_-}{R_o+X_o+R_L+j\omega_- \eta^1} \right) \right] \tag{43}$$

Transducer gain is defined as the ratio of the actual power output to the available power input. In Figure 6 the actual power output at ω_+ is $|I_+|^2 R_L$ and the available power input is $\frac{|V|^2}{4R}$.

Since

$$|V|^2 = \left\{ I_s \left[R + R_s + X_s + j\omega_s \left[\eta^1 + \eta_1^2 \left(\frac{j\omega_+}{R_o+X_o+R_L-j\omega_+\eta^1} \right) - \eta_1^2 \left(\frac{j\omega_-}{R_o+X_o+R_L+j\omega_-\eta^1} \right) \right] \right] \right\}^2 \tag{44}$$

and

$$I_+^2 R_L = I_s^2 \left[\frac{j\omega_+ \eta_1}{R_o+X_o+R_L-j\omega_+\eta^1} \right]^2 RL \tag{45}$$

the transducer gain at this frequency becomes

$$G = \frac{4\,RR_L\,I_+^2}{|V|^2} \tag{46}$$

$$= \frac{4\left\{\dfrac{j\omega_+ \eta_1}{R_o + X_o + R_L - j\omega_+ \eta^1}\right\}^2 RR_L}{\left\{R + R_s + X_s + j\omega_s\left[\eta^1 + \eta_1^2 \dfrac{j\omega_+}{R_o+X_o+R_L-j\omega_+\eta^1} - \eta_1^2\left(\dfrac{j\omega_-}{R_o+X_o+R_L+j\omega_-\eta^1}\right)\right]\right\}^2}$$

As an approximation assume that $\omega_+ \cong \omega_-$ and the gain becomes

$$G = \frac{(4\,RR_L)(-\omega_+^2)(\eta_1^2)}{(R + R_s + X_s + j\omega_s\eta^1)^2\ (R_o + X_o + R_L - j\omega_+\eta^1)^2} \tag{47}$$

Letting $R = R_s + X_s + j\omega_s\eta^1$ and $R_L = R_o + X_o - j\omega_+\eta^1$ the gain becomes

$$G = \frac{(-\omega_+^2)\eta_1^2}{(R_s + X_s + j\omega_s\eta^1)(R_o + X_o - j\omega_+\eta^1)} \tag{48}$$

Letting R_s, X_s, R_o and X_o be negligible produces a $G = \dfrac{\omega_+\eta_1^2}{\omega_s(\eta^1)^2}$ (49)

This gain is seen to approach the ratio of the output frequency to the input frequency as the coupling becomes better; showing the dependency of the gain of the device on the coupling obtainable. The theoretical gain is also the theoretical gain predicted by the Manley-Rowe relations.

Expressions for V_s^*, V_- and V_+^* are also obtained from the differentiation indicated by equation 37 and these equations plus the equations $V_s^* = I_s^*(R+R_s+X_s)$, $V_- = I_-(R_o+R_L+X_o)$ and $V_+^* = I_+^*(R_o+R_L+X_o)$ may be used to solve for the gain at ω_- in the same manner.

III. EXPERIMENTAL RESULTS

Physically implementing the balanced modulator illustrated in Figure 4 proved to be no simple task. The small size of the device and its components as well as the limited equipment available served to complicate the construction. The resultant model suffered from several disadvantages; exact alignment of the windings with respect to the film was not attained; the inductive coupling between the film and the signal and output windings was reduced by air gaps; the thin film did not become a single magnetic domain material, even under rather high bias fields, and as a consequence the sensitivity of the device was limited by Barkhausen noise.

The plated wire used in the modulator was rather small and it was not possible to determine if the rest direction of magnetization of the plated material was exactly circumferential to the axis of the wire. It is possible that some unbalance may have arisen at this point. The plated wire was dropped into the capillary tube so it would not be subject to strains that would introduce magnetostrictive effects. The output winding, made up of two coils each containing 200 turns of No. 44 wire, was wound on the outside of the capillary tube. It is apparent that the glass wall of the capillary and the air gap between the plated wire and the inner wall of the tube would reduce the coupling between the output winding and the film. The modulation or signal winding was made up of two coils each containing approximately 5000 turns of No. 52 wire. These coils were wound on "red fiber" coil forms that had holes through their center so they could be slipped over the output winding. Again a gap was introduced

by the walls of the coil form, the glass of the capillary, the output winding, and the air that separated the modulation winding from the film. While each winding was centered around the capillary tube and the inside diameter of the tube was made as small as possible, there were still spaces present that may have been sources of misalignment. By having the output windings wound in opposite directions some of the effects of improper alignment would be canceled.

The carrier frequency power was supplied by a crystal controlled vacuum tube oscillator operating at 5.5 mc/s. This value is not critical. A rather high frequency was selected primarily because of the advantage in power gain that would result, but a disadvantage in using a higher frequency is the closer coupling that would exist between the carrier and the output winding due to the interwinding capacitance.

Conventional vacuum tube and transistor power supplies were used for the carrier oscillator and the various bias currents used, but at low levels it was found that these sources introduced an appreciable amount of noise into the system. Therefore, for low level measurements, it was necessary to use a battery to supply power for the vacuum tube filaments and the d-c bias currents in the carrier and the modulation windings.

As was mentioned d-c bias currents were used in both the carrier and the modulation windings. A d-c bias current in the carrier winding maintains the film in a single magnetic domain and tends to align the magnetization vector, $\vec{M}$, in the same direction as the magnetic field of the carrier winding. A d-c bias current in the modulation winding can be used to correct for misalignment with respect to the modulation winding

to obtain a more nearly balanced output.

Stray field effects such as that of the earth's magnetic field tend to be disturbing or helpful depending upon their usage. Sometimes the earth's field may be used to supply a portion or all of the d-c bias field that maintains the film in a single magnetic domain, but this is not an entirely satisfactory arrangement. The most suitable situation is to effectively shield the device with a high permeability material so external fields will have no effect and all of the other fields used in the modulator are controllable.

If it is assumed that all external sources of noise have been eliminated and that the device operates as a true balanced modulator the only noise source known to exist in the modulator itself would be modulated thermal agitation noise. The currents that flow as a function of thermal agitation affect the modulator in exactly the same way as do signal currents.

Some external sources of noise that may be present are:

(a) Noise produced by the exciting oscillator.

(b) Noise arising in the amplifier following the modulator.

(c) External stray field effects.

(d) Thermal currents that would arise from resistive elements in the system.

Basically the balanced modulator is a small signal device. Samuels (9) has shown that the modulator becomes extremely nonlinear as the modulation current is increased beyond certain limits. Since the primary purpose of this study was to investigate the thin film balanced modulator in the low level, low frequency range, measurements were limited to the

linear region of operation.

The open circuit voltage output of the modulator as a function of the input voltage is given in Figure 7. The voltage gain is seen to be small, on the order of 1.44. The output is linear for input voltages from 0 up to approximately 6 volts peak to peak. Beyond this the output shows some distortion. Substantially identical open circuit characteristics were obtained at 100 and 1000 cps.

The effect of resistive loading on the modulator was measured at three frequencies (10, 100, and 1000 cps) to determine the apparent output impedance. The results are shown in Figure 8. Two of the measurements were begun with output voltages of 4.6 volts while the third measurement was begun at 2.5 volts. Inspection of these curves indicates that the output impedance is relatively small and approximately the same for the three frequencies. Since the d-c resistance of the output coil is approximately 9.37 ohms and the output impedance is about 200 ohms, most of the impedance is reactive; as is suggested by the Thevenin equivalent impedance derived earlier. The Thevenin equivalent impedance was not a function of signal frequency and did not consider any loss mechanisms. The value of 200 ohms measured amounts to the approximate value of impedance ascribable to the air inductance of the output coil.

The output of this particular modulator with two different resistive loads (1000 and 10,000 ohms) was measured to determine its range of operation as a function of frequency. The results are given in Figure 9. It is seen to have a bandwidth of about 20,000 cps starting at d-c. The upper cut-off frequency is determined by the inductance of the input coil.

Figure 7. Open circuit output voltage of the amplifier as a function of the input voltage.

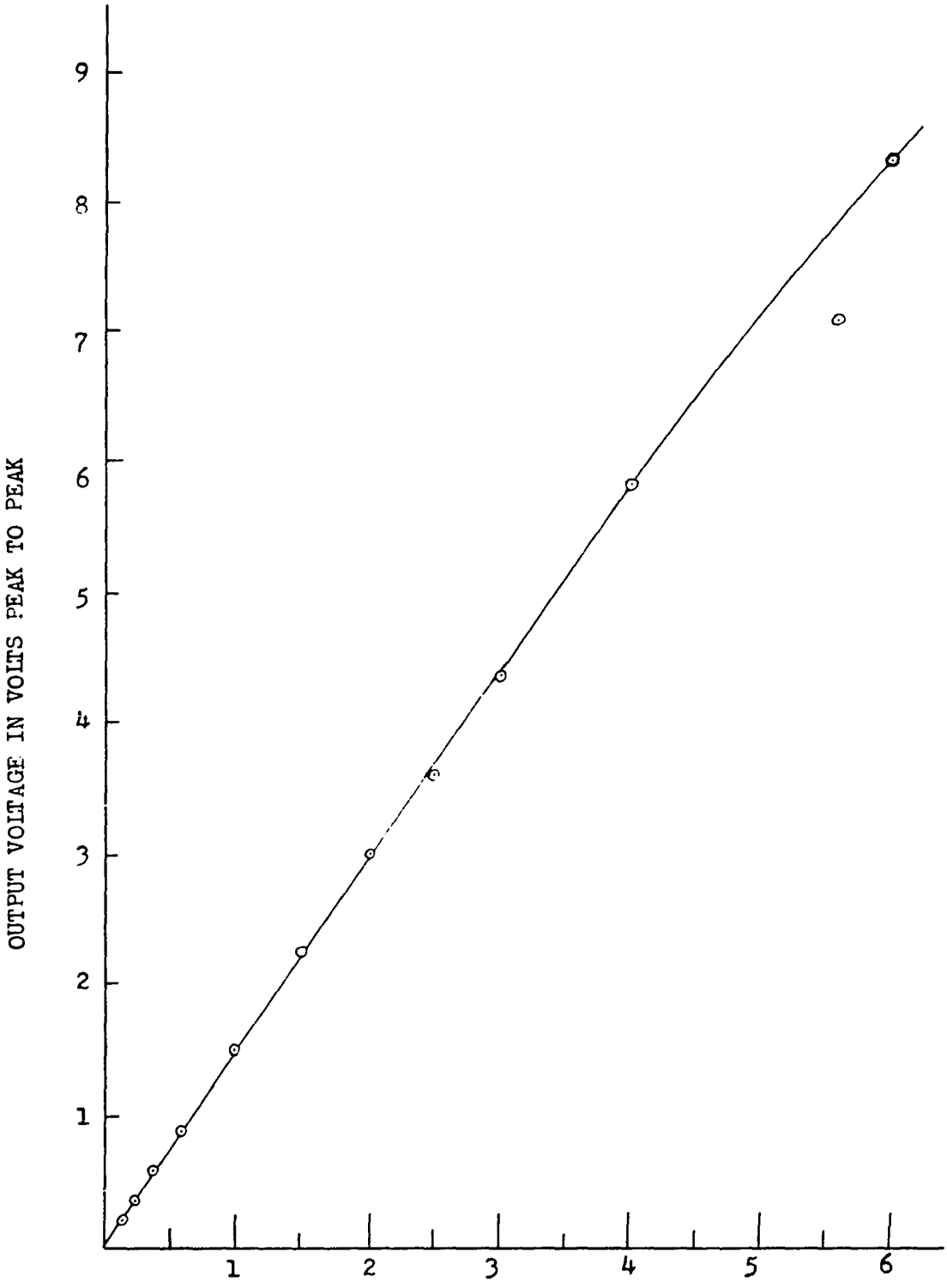
OUTPUT VOLTAGE IN VOLTS PEAK TO PEAK
9
8
7
6
5
4
3
2
1
1
2
3
4
5
6
INPUT VOLTAGE IN VOLTS PEAK TO PEAK

Figure 8. Output voltage of the amplifier as a function load resistance for two different initial voltages and three different frequencies.

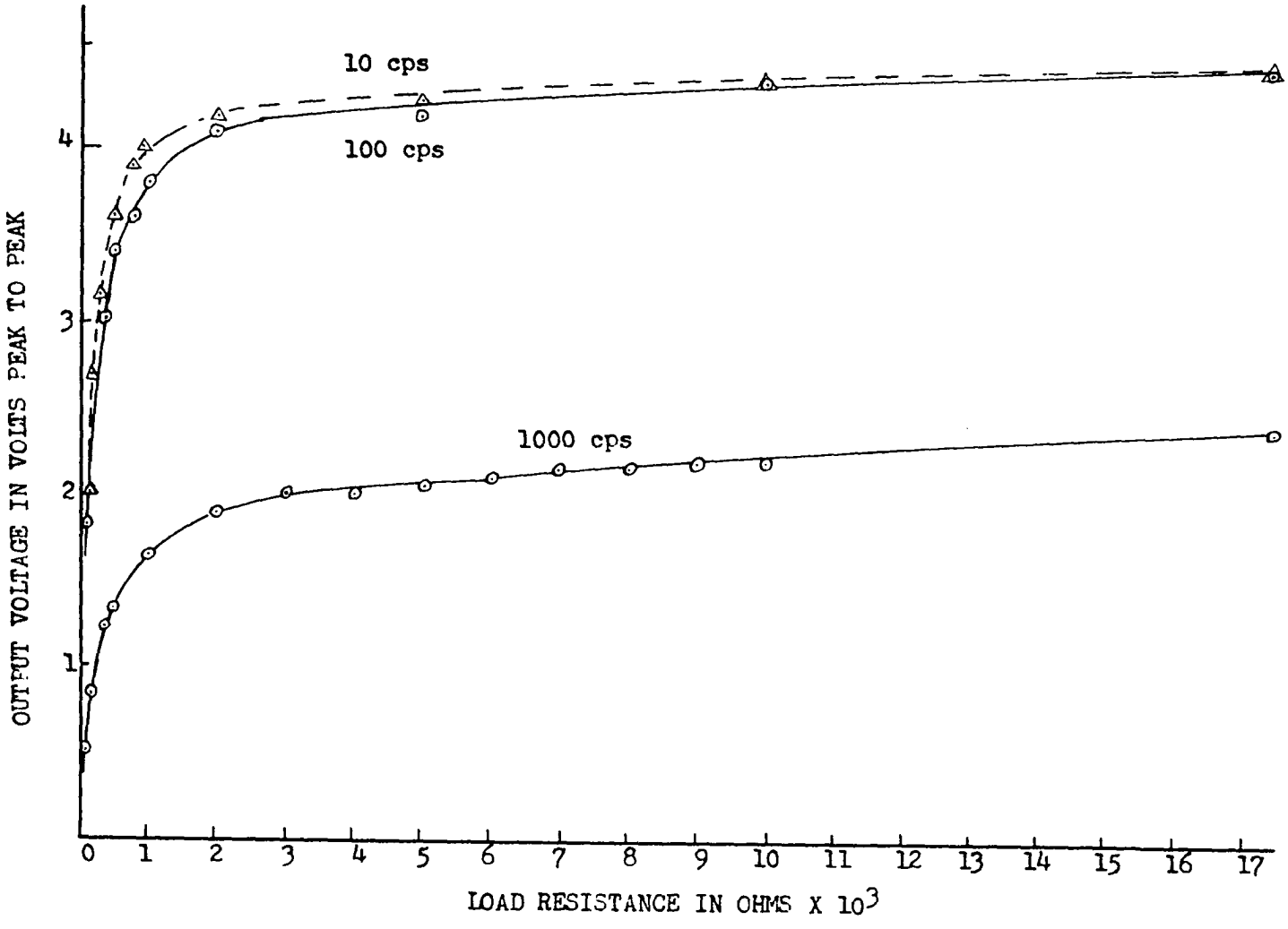
10 cps
100 cps
1000 cps
OUTPUT VOLTAGE IN VOLTS PEAK TO PEAK
1
2
3
4
0 1 2 3 4 5 6 7 8 9 10 11 12 13 14 15 16 17
LOAD RESISTANCE IN OHMS X 10^3

Figure 9. Output voltage of the amplifier as a function of frequency.

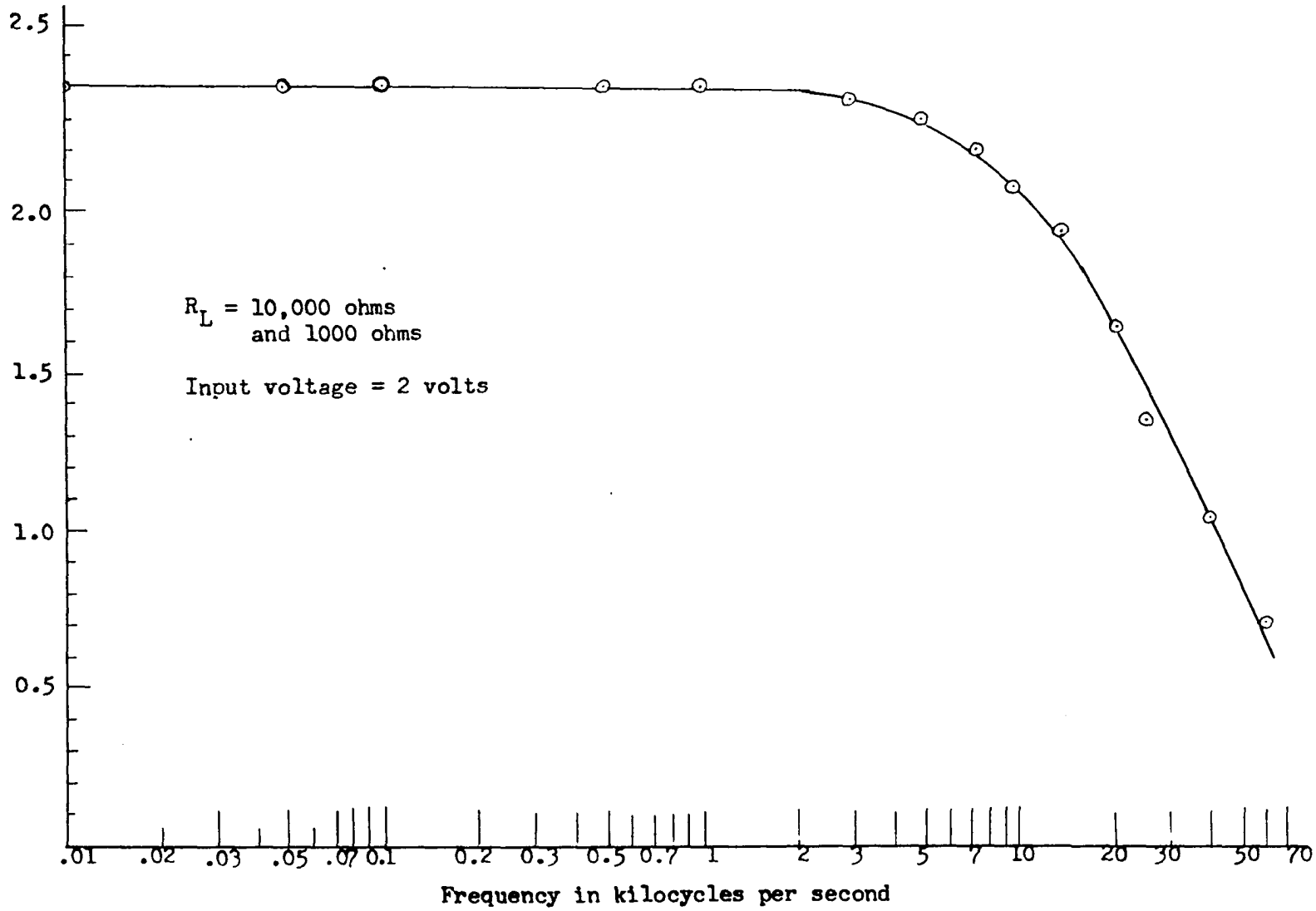
2.5
2.0
1.5
1.0
0.5
R_L = 10,000 ohms
and 1000 ohms
Input voltage = 2 volts
.01
.02
.03
.05
.07
0.1
0.2
0.3
0.5
0.7
1
2
3
5
7
10
20
30
50
70
Frequency in kilocycles per second

Current gains of 21.65 and 4.75 were obtained with two different types of resistive loads. The higher gain occured with what was approximately a matched load of 170 ohms at 100 cps, while the lower gain resulted with a relatively light load of 1000 ohms at two frequencies (100 and 1000 cps). While the increased load seems to have a point in its favor with the higher current gain, the useful range of signal input was limited by the distortion in the output at the larger signals levels. The distortion probably appears when the field effects of the current in the output winding become large enough to influence the operation of the modulator.

Different methods were used to demodulate the output of the balanced modulator. The first utilized a vacuum tube as a mixer followed by a low-pass filter. In addition to the mixing action an amplification of the signal input is also realized by the use of this method. The resultant voltage gain of the system came to 15.3 as compared to the voltage gain of 1.44 from the modulator alone. A disadvantage that attended the use of the vacuum tube was that at a low level signal input some noise appeared in the output. This noise was eventually traced to the filament of the tube. It is possible that the noise could have been reduced to a negligible value by the use of a battery to supply the filament power. Another method of demodulation involved the use of transistors in a linear adder and the subsequent filtering of the output from the adder. This system was more satisfactory for a low signal input condition but the voltage gain obtainable was only 2.29 and the magnitude of the input signal that could be handled was reduced considerably by the limitations of the adder circuit. A low noise amplifier was designed and cascaded

Figure 10. Output current of the amplifier as a function of input current at a matched load (170 ohms) and a load of 1000 ohms.

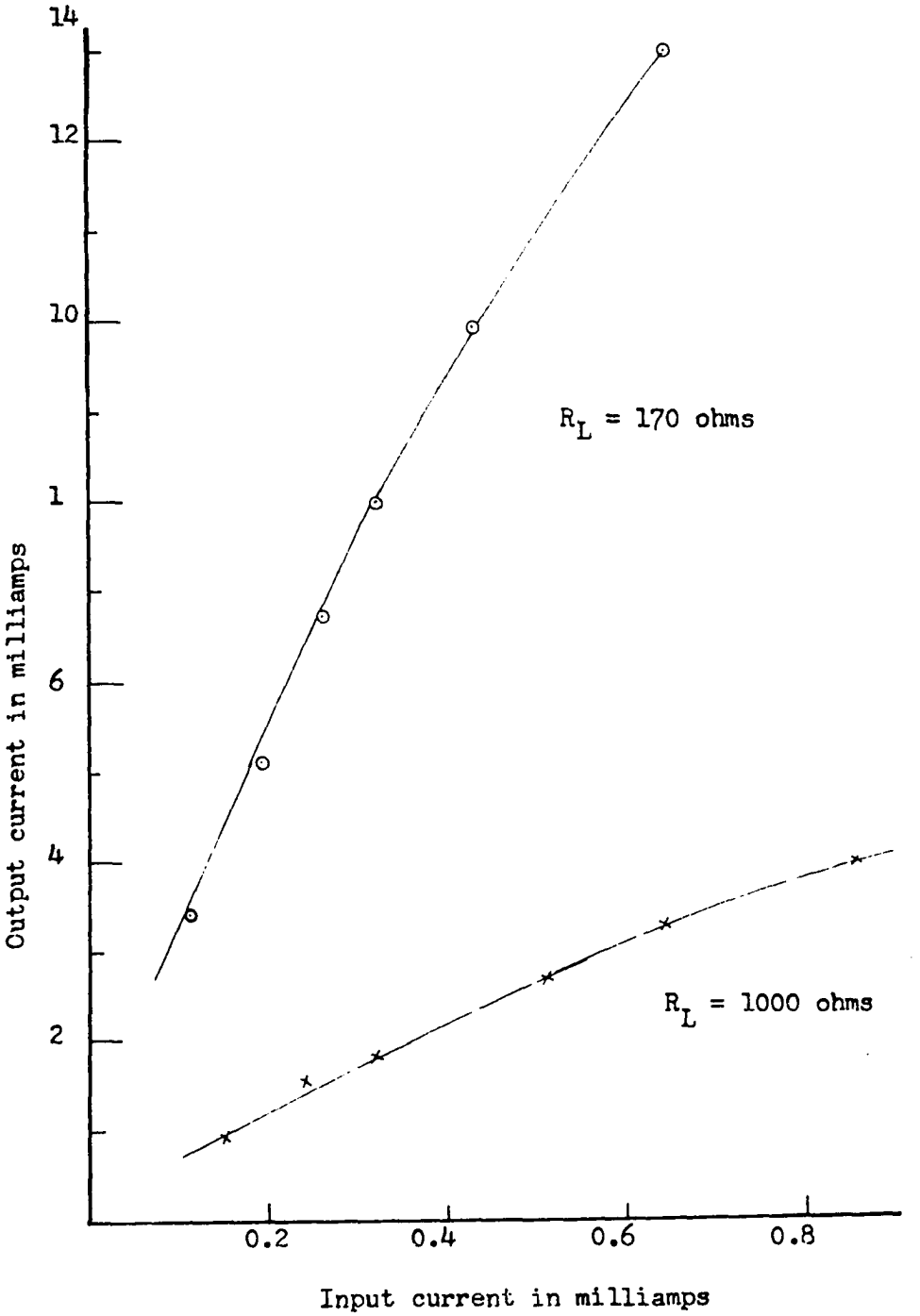
14
12
10
1
6
4
2
Output current in milliamps
R_L = 170 ohms
R_L = 1000 ohms
0.2
0.4
0.6
0.8
Input current in milliamps

with two commercial amplifiers to obtain a noise measurement of the modulator. The noise output of this arrangement, illustrated in Figure 11, proved to be negligible when it was compared to the noise of the modulator.

As was mentioned the plated film did not exist as a single magnetic domain and as a consequence considerable noise was introduced by the Barkhausen jumps that occured when the domain walls shifted. That the noise did come from Barkhausen jumps may be deduced by consideration of the data plotted in Figure 12. The graph is a plot of the noise figure of the device as a function of d-c bias current in the carrier winding. As the d-c bias current was increased the magnetization of the film more closely approached the ideal condition of a single magnetic domain, or consisted of fewer domains. These results are similar to those obtained by Williams and Noble (12) in their analysis of the Barkhausen noise present in the second-harmonic type of magnetic modulator using bulk ferromagnetic cores. Thus, the sensitivity of the model used in these experiments is limited by Barkhausen noise and that to achieve the low-level, low-noise amplification hoped for it would be necessary to have single domain magnetic material.

The average noise figure obtained in measurements on this modulator is seen to be in the order of 2×10^3. This is so large that it is almost ridiculous, but it does serve to illustrate the extreme sensitivity of the device. For noise measurements under ideal conditions the only input to the modulator would have been that equivalent to the thermal noise that would be added by the noise generator's internal resistance, with the actual output of the noise generator equal to zero. However, when the

Figure 11. Equipment used in making noise measurements. (A) The magnetic thin film parametric amplifier, a low noise transistor amplifier and a detector. (B) A block diagram of the equipment used in making noise measurements on the parametric amplifier.

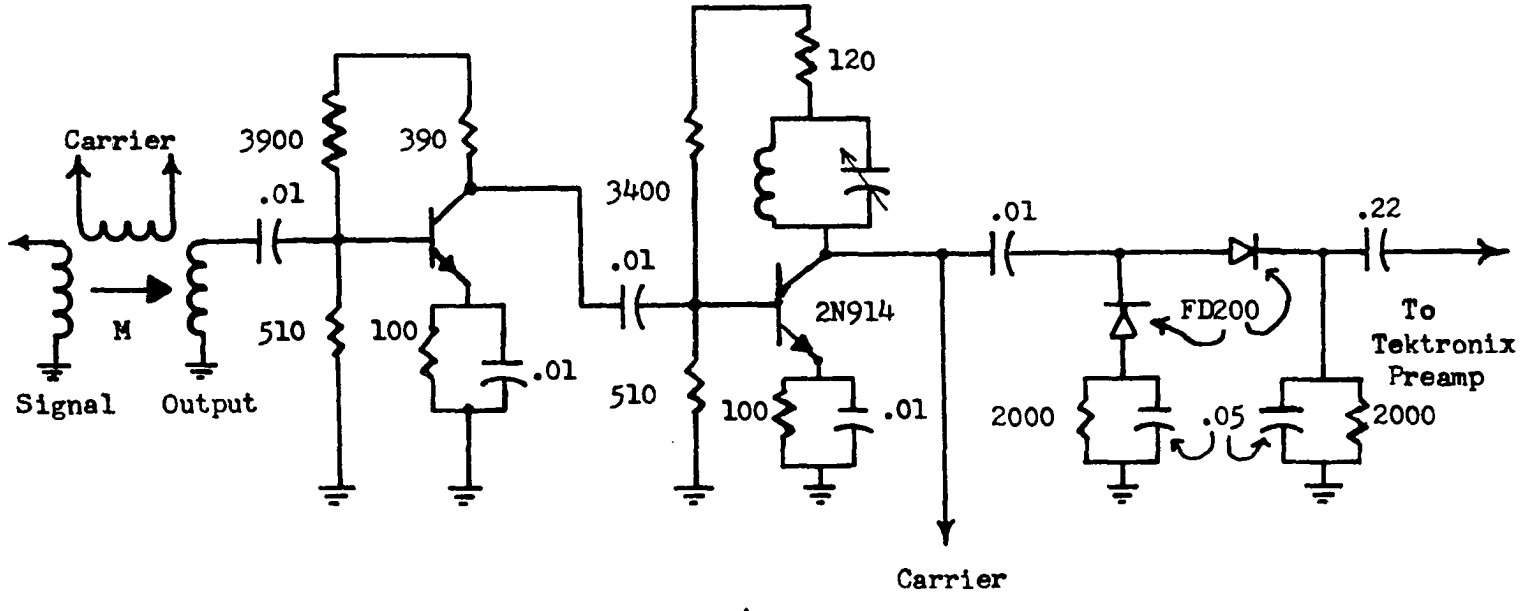
Carrier
3900
390
.01
120
3400
.01
.01
.22
2N914
FD200
To
Tektronix
Preamp
M
510
100
.01
Signal
Output
510
100
.01
2000
.05
2000
Carrier

A

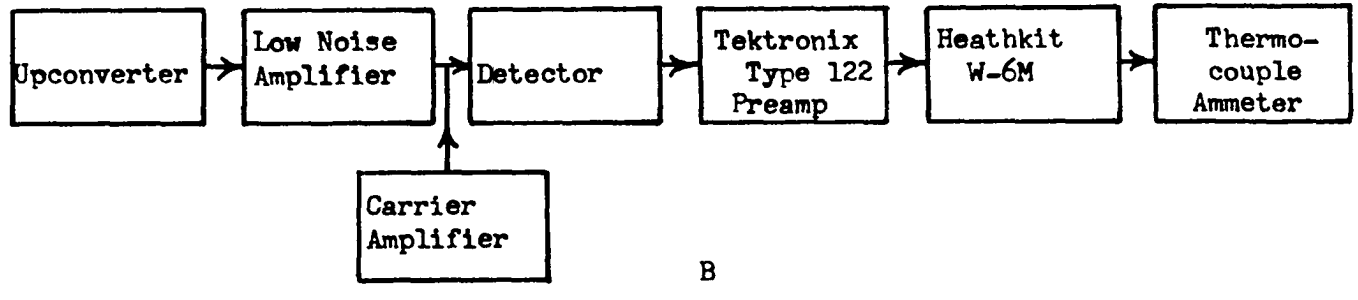
Upconverter
Low Noise
Amplifier
Detector
Tektronix
Type 122
Preamp
Heathkit
W-6M
Thermo-
couple
Ammeter
Carrier
Amplifier

B

Figure 12. Average noise figure measured, using the system illustrated in figure 11B, as a function of d-c bias current in the carrier winding.

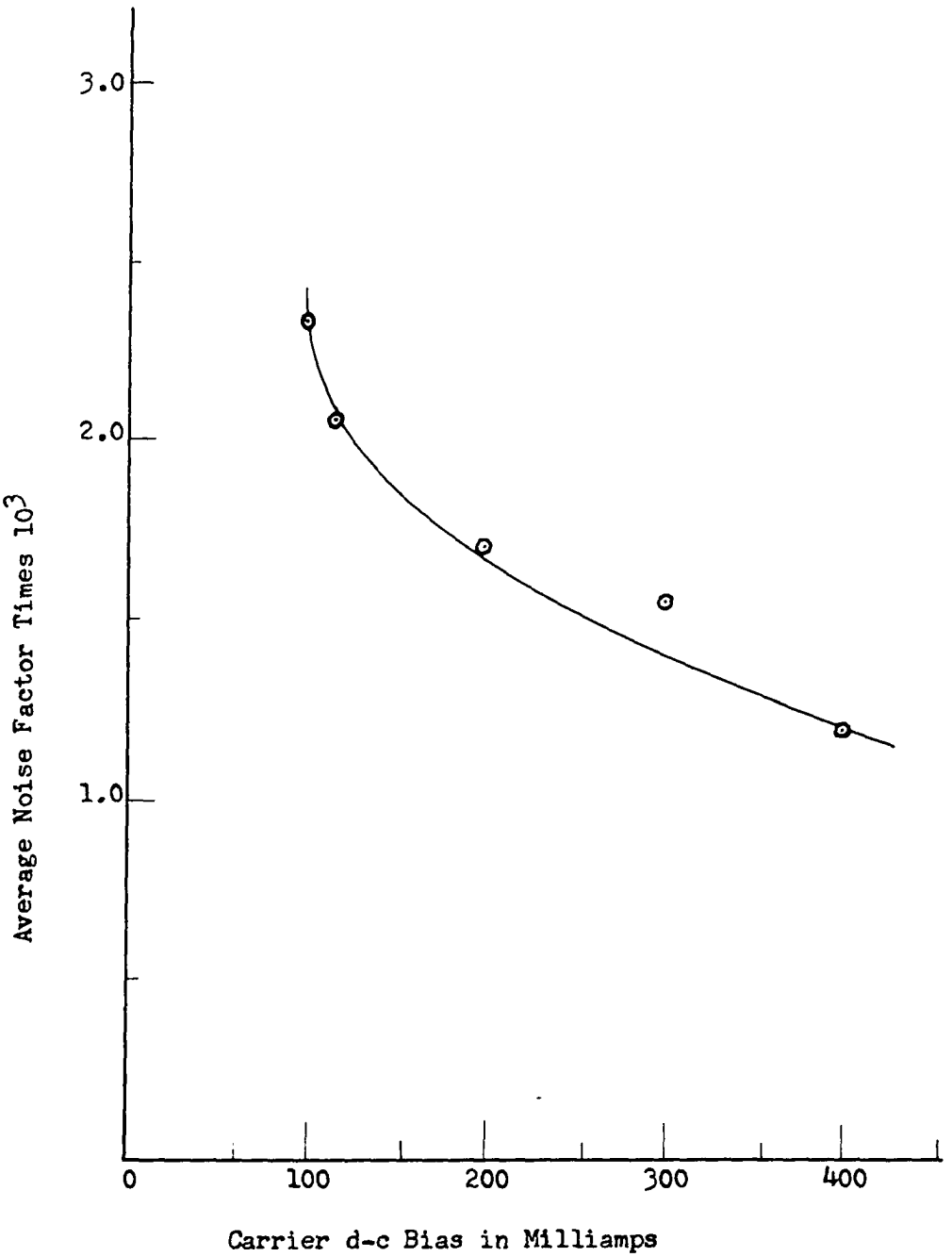
3.0
2.0
1.0
Average Noise Factor Times 10^3
0
100
200
300
400
Carrier d-c Bias in Milliamps

measurements were made, additional inputs were detected coming from such sources as the 60 cycle magnetic fields in the building etc. While these effects themselves were large enough to appear in the output of the device and add to the "noise", they also probably increased the Barkhausen noise content mentioned earlier. Until the effects of these stray fields may be eliminated the true noise figure of the amplifier cannot be measured.

As a result of the demonstrated ability of the up-converter to detect weak magnetic fields an experiment was made to get a feel for its suitability for use as a magnetometer. While the measurement was rather crude and there was a degree of canceling because the output windings were wound in opposite directions, a change in field strength of approximately 5×10^{-5} oersted was detected. There is good reason to believe that better sensitivities could be attained if a thin film up-converter were designed specifically for this application.

IV. DISCUSSION

The results of this investigation indicate that the thin film balanced modulator can become a very useful tool as an up-converter amplifier for low-level, low-frequency, low-noise applications. There is a need for devices of this nature. It should prove to be rugged, stable and sensitive, with a sensitivity that is limited only by inherent thermal noise.

Future studies on this particular type of modulator should probably be made in obtaining experimental results concerning the applicability of the equivalent circuit that has been developed. Other studies could investigate the application of an array of these up-converters in magnetic field sensing devices.

The most important work to be done before any of these applications of the thin film inductor will be fruitful lies in the area of fabrication. The necessity for single domain magnetic material has been illustrated in this study, and the problems of proper alignment of the various windings and the film have been mentioned before. Since these items are so critical in the operation of the balanced modulator and the up-converter amplifier, and since the material and the windings are so small, probably the only way to solve these problems is some form of machine of assembly. In any event a good deal of work in the fabrication techniques necessary to produce these devices is still needed.

V. BIBLIOGRAPHY

1. Biorci, G. and Pescetti, D. Frequency spectrum of the Barkhausen noise. Journal of Applied Physics 28: 777-780. 1957.

2. Fonger, W. H. Noise in transistors. In Smullin, L. D. and Haus, H. A., eds. Noise in electron devices. pp. 344-405. New York, N.Y., John Wiley and Sons, Inc. 1959.

3. Ford, N. C. and Pugh, E. W. Barkhausen effect in nickel-iron films. Journal of Applied Physics 30: 270S-271S. 1959.

4. Manley, J. M. and Rowe, H. E. Some general properties of nonlinear elements. I. General energy relations. Proceedings of the Institute of Radio Engineers 44: 904-913. 1956.

5. Nyquist, H. Thermal agitation of electric charge in conductors. Physical Review 32: 110-113. 1928.

6. Read, A. A. Electronic applications of magnetic films. Unpublished Ph. D. Thesis. Ames, Iowa, Library, Iowa State University of Science and Technology. 1960.

7. _____ and Pohm, A. V. Magnetic film parametric amplifiers. Proceedings of the National Electronics Conference. (1959) 15: 65-78. 1960.

8. Salzberg, B. Masers and reactance amplifiers; basic power relations. Proceedings of the Institute of Radio Engineers 45: 1544-1545. 1957.

9. Samuels, R. L. Thin ferromagnetic film balanced modulators. Unpublished M.S. Thesis. Ames, Iowa, Library, Iowa State University of Science and Technology. 1960.

10. Tebble, R. S. The Barkhausen effect. Proceedings of the Physical Society 68: 1017-1032. 1955.

11. Van Der Ziel, A. Low-frequency noise in vacuum tubes (flicker effect). In Smullin, L. D. and Haus, H. A., eds. Noise in electron devices. pp. 45-76. New York, N.Y., John Wiley and Sons, Inc. 1959.

12. Williams, F. C. and Noble, S. W. The fundamental limitations of the second-harmonic type of magnetic modulator as applied to the amplification of small D.C. signals. Proceedings of the Institution of Electrical Engineers 97, Part 2: 445-459. 1950.

VI. ACKNOWLEDGEMENTS

The writer wishes to express his appreciation to his major professor, Dr. A. V. Pohm, for suggesting the topic and for his helpful comments and suggestions.

The writer also wants to thank Mr. A. J. Stattelman for his help and suggestions in the experimental work, Mrs. Vernon L. (Judy) Worrell for the typing of the manuscript, and other members of the Department of Electrical Engineering for their interest and comments and his family for their understanding and encouragement.

VII. APPENDIX

A. Thermal Noise

Given two resistors in thermal equilibrium at temperature T and connected together as shown in Figure 13A the energy generated in R_1 by the random motion of charges will be absorbed by R_2, and that generated in R_2 will be absorbed by R_1. Since the resistors are in thermal equilibrium, the power flowing from R_1 to R_2 must equal the power flowing from R_2 to R_1. In addition to the requirement that the energy being exchanged between the resistors be equal it is also necessary that the energy exchanged between the two resistors must be in equilibrium for every infinitesimal frequency range df. If this condition did not hold it would be possible for one resistor to extract heat from the other by the use of a nondissipative band-pass filter. Because both resistors are initially at the same temperature such an exchange of power would contradict the second law of thermodynamics.

The next step is to consider an infinite length of transmission line and to restrict the energy transfer to a given frequency band, df, in which only the lowest mode can be propagated. (This would correspond to the principal of the coaxial line or the dominant mode of a wave guide). When the transmission line is in thermal equilibrium at temperature T, it will store electromagnetic energy in a given unit of its length in a manner similar to the storage of heat energy in a given volume of gas at a temperature T. The heat energy of a gas arises from the random motion of its molecules, while the heat energy of the transmission line will appear in electromagnetic waves of random phase traveling back and

Figure 13. Circuits used in the accompanying derivation of the thermal emf present in (A) a resistor and (B) an impedance at a given temperature T.

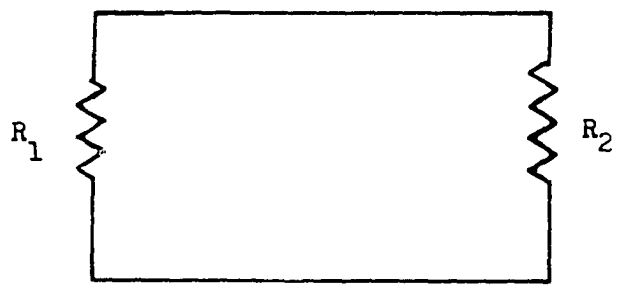

A

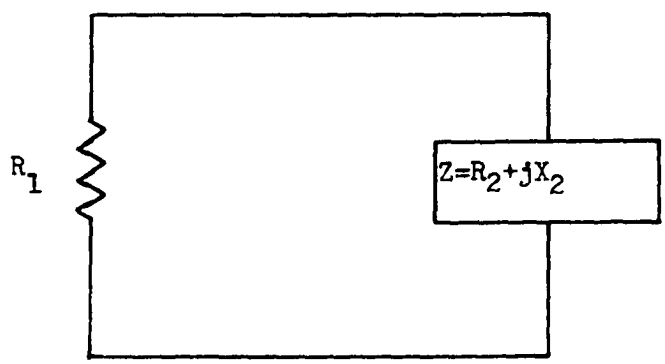

B

forth in the transmission line. It can be shown that the average stored electromagnetic energy per unit length of line equals $2(kT/c)df$ where k is Boltzmann's constant, T is the temperature in degrees Kelvin, c is the velocity of light and df is the frequency range in question. Since the energy is traveling to the left and to the right at the velocity c, the energy flow through a cross section of line will be equal to that stored in a section of the line c meters long. From this it follows that the power flow to the right or to the left in the frequency range df will be kTdf since half of the power stored in a given section of line will be flowing in each direction.

If the resistors R_1 and R_2 are connected at either end of a finite section of the transmission line described above and all those elements are at temperature T it is also necessary that there be an equilibrium of energy transfer in very infinitesimal frequency band.

Allow the resistors R_1 and R_2 to have the property of absorbing all energy incident upon them from the line. This would correspond to letting the resistors be equal to the characteristic impedance of the line or wave guide and they would then be electrically equivalent to an infinite length of transmission line. With all of the elements in thermal equilibrium the transmission line will still have the same electrical properties discussed before and power in the frequency range df equal to kTdf will be flowing to the right and to the left. This requires that R_1 and R_2 each absorb power kTdf in this frequency range. The condition that R_1 and R_2 are in thermal equilibrium with the line and with each other requires that both R_1 and R_2 must also radiate power kTdf in the frequency range df. The power absorbed by R_1 in the frequency range df may be

assumed to arise from an emf, e_2, originating in R_2. For the matched impedance condition $R_1 = R_2$ and the current through R_1 equals $\frac{e_2}{2R_1}$. The power absorbed by R_1 equals $R_1 \left(\frac{e_2}{2R_1}\right)^2 = \frac{\overline{e_2^2}}{4R_1} = kTdf$. Therefore $\overline{e_2^2} = 4R_1kTdf$. Or the effect of electrical fluctuations caused by a resistor R at uniform temperature T is equivalent to that of an emf, e_2, whose mean square value is $4RkTdf$ in the frequency range df.

This approach may now be expanded to the case of a resistor connected to an impedance as is shown in Figure 13B. The two elements are assumed to be at a uniform temperature T. The power absorbed in R_1 is equal to the power transferred to Z by R_1, and the power absorbed by Z is equal to the power transferred by Z to R_1 in keeping with the equilibrium condition. The power absorbed by Z from R_1 equals

$$R_2\left[\frac{\overline{e_1^2}}{(R_1+R_2)^2 + X_2^2}\right] \qquad \text{A1}$$

and the power absorbed by R_1 from Z equals

$$R_1\left[\frac{\overline{e_1^2}}{(R_1+R_2)^2 + X_2^2}\right] \qquad \text{A2}$$

Equating these two powers and solving for $\overline{e_2^2}$ gives

$$\overline{e_2^2} = 4kTR_2df \qquad \text{A3}$$

or the effect of thermal noise in an impedance $Z = R_2 + jX_2$ is equivalent to an emf e_2 in series with a noiseless Z; with the mean square value of e_2 being equal to $4kTdf$ times R_2 or the effective series resistance of Z at the frequency in question.